

TDOA for Narrow-band Signal with Low Sampling Rate and Imperfect Synchronization

Zan Li*, Desislava C. Dimitrova*, David Hawes Raluy*[†], Torsten Braun*,

* Institute of Computer Science and Applied Mathematics, University of Bern, Bern – Switzerland

[†] Barcelona School of Telecommunications Engineering, Polytechnic University of Catalonia, Barcelona – Spain

Email: li@iam.unibe.ch, dimitrova@iam.unibe.ch, david.saeed.hawes@alu-etsetb.upc.edu, braun@iam.unibe.ch

Abstract—Time-based localization techniques such as multilateration are favoured for positioning to wide-band signals. Applying the same techniques with narrow-band signals such as GSM is not so trivial. The process is challenged by the needs of synchronization accuracy and timestamp resolution both in the nanoseconds range. We propose approaches to deal with both challenges. On the one hand, we introduce a method to eliminate the negative effect of synchronization offset on time measurements. On the other hand, we propose timestamps with nanoseconds accuracy by using timing information from the signal processing chain. For a set of experiments, ranging from sub-urban to indoor environments, we show that our proposed approaches are able to improve the localization accuracy of TDOA approaches by several factors. We are even able to demonstrate errors as small as 10 meters for outdoor settings with narrow-band signals.

I. INTRODUCTION

Localization and tracking have emerged in recent years as an attractive solution to enable new business models that rely on personalized provisioning of location-based services. Different radio technologies can be applied for localization but their suitability depends on the environment context, e.g., outdoor, indoor. The Global Positioning System (GPS) can generally provide accurate outdoor location information but its usability is limited to areas with clear view to satellites. Therefore, multiple positioning approaches relying on radio technologies such as GSM and WiFi have been proposed for localization in dense urban areas and indoor spaces [1]. We select to work with GSM signals due to the wide GSM adoption by end users, who we are interested to localize. In our work, we aim to passively overhear GSM uplink signals and apply localization algorithms to find a user's position.

Ranging via the Time Difference of Arrival (TDOA) method is among the most promising proposals. In TDOA the tracked object is positioned relative to at least three Anchor Nodes (ANs) with known coordinates. The ANs overhear transmissions from the target and calculate a location estimated by comparing differences in the arrival times (represented by timestamps). The performance of TDOA depends on two time-related aspects. First, it is critical that the ANs are synchronized with nanoseconds accuracy. Currently available synchronization schemes can typically deliver accuracy in the order of milliseconds or microseconds [2]. GPS as a synchronization option is more promising with theoretically expected performance in the order of nanoseconds. However, in our previous work to evaluate GPS synchronization, we

demonstrated a remaining offset of 200ns, which may not be satisfying for TDOA and should be taken into account in practice. Second, high resolution timestamps are an essential precondition for TDOA ranging with few meters accuracy. The narrow-band property of the GSM signal poses difficulties to take accurate timestamps because of the long symbol duration. The problem is aggravated by multipath propagation and shadowing, since the multiple signal components arriving via different paths can severely distort the symbol [3].

In this paper we propose approaches to tackle both synchronization and accurate timestamps. First, we propose a method to eliminate the impact of imperfect node synchronization. Our analysis of GPS synchronization shows that it still leaves a minor offset with unpredictable variation. We propose to use Differential TDOA (DTDOA), which introduces a Reference Node (RN) to the TDOA technique, to compensate the momentary synchronization offset and eventually increase the positioning accuracy. Second, we offer an analytical model to formally describe the time components of TDOA and the proposed DTDOA method. Furthermore, inspired by information from signal processing at the physical layer, we introduce a new high-resolution physical-layer timestamp for narrow-band signals (e.g., GSM). The timestamp can be taken with accuracy of nanoseconds. Finally, we conduct evaluations for three different environments, i.e., sub-urban, urban and indoor, and demonstrate the positioning accuracy achieved by TDOA and DTDOA. We show that the DTDOA approach is able to reach 10m localization accuracy in sub-urban environments.

In Section II we first discuss the challenges and related works in TDOA localization. Our first contribution about the TDOA modeling and compensation of the GPS synchronization offset with DTDOA is presented in Section III. Section IV introduces the second contribution, methods to increase the timestamp resolution. Implementation and measurement setup are introduced in Section V, followed by Section VI, which presents and analyzes the measurement results. Finally, Section VII concludes the paper.

II. CHALLENGES AND RELATED WORK ON TIME-BASED LOCALIZATION

Time-based localization relies on time measurement of the RF signal to derive the location of the target. The time measurements are taken at several ANs and represented by timestamps. Two factors, i.e., anchor nodes synchronization and timestamp accuracy, influence the localization accuracy, and are discussed in the following subsections.

A. Anchor Nodes Synchronization

Owing to the high propagation speed of radio signals, time-based localization requires strict synchronization between the ANs. For instance, synchronization inaccuracy as small as $100ns$ can result in a localization error as big as $30m$. Among the many node synchronization proposals, GPS synchronization provides a state-of-the-art solution with theoretical studies showing nanosecond accuracy. Indoor ANs can be synchronized by GPS receivers with outdoor antennas.

In our previous work [4], GPS synchronization was evaluated against the requirements of TDOA. Figure 2 shows the variation of GPS synchronization, where the blue curve indicates the GPS synchronization offset between two ANs in 12 hours and the red curve is the synchronization offset in 20 seconds with the maximum measured clock skew. We found that even if two GPS receivers are co-located and receive the signal from the same satellites, there is still a remaining synchronization offset. Although a maximum offset value of $423ns$ was measured, most offsets were within $200ns$, corresponding to $60m$ localization error. Taking into account that the synchronization offset is influenced by lost connection to the satellites [5], the distribution of the synchronization offset becomes unpredictable.

Research has been done to solve imperfect synchronization. DTDOA using a RN has been discussed in [6] for Wireless LAN systems. The authors evaluated their approach in a MATLAB simulation but no evaluation in real world is done. In practice, the authors of [7] demonstrated that some limitations are posed on the interval between the transmissions of the RN and the target, denoted by I_{TR} as shown in Figure 1(b). Since the RN can not transmit simultaneously with the target, certain synchronization drift between the non-perfectly synchronized ANs will accumulate during the interval I_{TR} . According to [7] the accumulated synchronization drift within I_{TR} can introduce ranging errors as large as $250m$ in a practical system. The authors proposed to estimate the mean clock drift between two unsynchronized local clocks in an off-line phase and to compensate the accumulated synchronization drift during the on-line phase. However, they also showed that the momentary clock drift varies randomly from the mean value, demanding very short I_{TR} , e.g., hundreds of microseconds, to meet the strict requirements of TDOA localization.

B. Timestamp Accuracy

In a deployed wireless network the timestamp for the received message reflects the signal propagation time as well as the processing time spent at the transmitter and the receiver [2]. While the processing time at the transmitter is the same for all ANs, the time at the receivers may differ. Typically, a timestamp is given at the MAC layer and the accuracy is only on the microseconds level because of processing delay at physical and MAC layers [8]. Consequently, a timestamp is best given close to the physical layer to avoid influences from processing time at the MAC or higher layers at the receiver. At physical layer, a conventional timestamp [9] is a sample-based timestamp, which is defined as the hardware-given timestamp when a sample of a packet is received at the RF frontend.

The accuracy of a physical layer timestamp is highly dependent on the signal's bandwidth. Most studies on TDOA

with RF signal focus on Ultra Wide Band (UWB) signals [3]. Due to the wide bandwidth (larger than $500MHz$), UWB can achieve nanosecond accuracy for sample-based timestamps. However, for signals with more narrow bandwidth, the accuracy of sample-based timestamps would be lower. For example, the GSM signal with bandwidth of $200KHz$ results in a coarse time resolution of $5\mu s$ ($1.5km$ in distance). Hence, a sub-sample timestamp, which is able to estimate the time difference within one sample interval, should be designed to improve the accuracy in case of narrow-band signals.

Complex indoor propagation is another aspect limiting the accuracy of TDOA. The sources of errors include multipath propagation and shadowing. The radio signals reaching the receiving antenna via different paths result in multipath propagation. Benefiting from its wide bandwidth and correspondingly extremely short pulse interval, UWB can resolve and separate the multipath components [3]. However, for a narrow-band system, the signals from different paths would overlap in one symbol duration, making the detection of the direct path nontrivial. Furthermore, shadowing would attenuate or completely block the direct path, adding another bias to the range estimate. The authors of [10] analyzed TDOA performance with GSM signals in simulation and provide accuracy of $11.4m$ in Line Of Sight (LOS) situations and $23.3m$ in Non Line Of Sight (NLOS) situations with $200KHz$ bandwidth. They do not consider, however, practical factors such as synchronization and sampling rate. TruePosition is a leader in the deployment of location technologies in support of the E911 mandate. They provide Uplink-TDOA (U-TDOA) solution for GSM localization. The accuracy is influenced by the mentioned factors, i.e., AN synchronization and multipath propagation, and they declared the localization accuracy from $50m$ to $150m$ in urban and sub-urban environments in their report [11].

III. LOCALIZATION ALGORITHMS

In this section, we propose new analytical models for TDOA and DTDOA. At the same time, we also provide a mechanism to combining DTDOA and GPS synchronization in order to compensate for the synchronization offset.

A. TDOA Model

TDOA is defined as the difference of arriving times between ANs for the same packet from the target. Based on the factors influencing the accuracy of TDOA, we propose to decompose TDOA into four components as follows,

$$TDOA = T_d + T_{sh} + T_{sy} + n, \quad (1)$$

where $TDOA$ is overall TDOA value, T_d is the TDOA component related to the geometric distance, which is defined as distance component, T_{sh} is the shadowing and multipath component, T_{sy} is the synchronization offset component and n is Gaussian noise. Among those components, only T_d is related to the actual distance, while the others introduce timing errors.

The components T_d and T_{sh} are determined by the position of the target, and thus they are space-determined components. Therefore, in a static environment with fixed position of the target, T_d and T_{sh} would be constant. Then, given the Gaussian

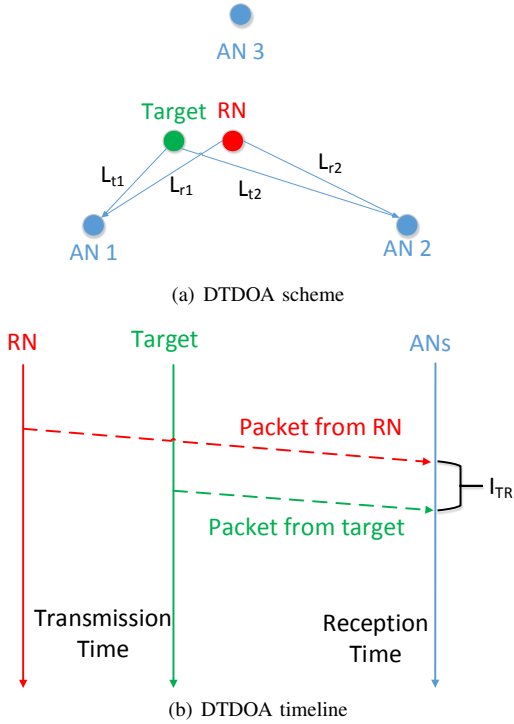


Fig. 1: Differential time difference of arrival

distribution of the noise component n and abstracting T_{sy} from $TDOA$, the distribution of $T_d + T_{sh} + n$ is Gaussian distribution with the mean value of $T_d + T_{sh}$.

As introduced in Section II-A, our previous work [4] concluded that the component T_{sy} with GPS synchronization is unpredictably variant with time and is not a space-determined component. Assuming that the synchronization component is independent from the other components, the distribution of the overall $TDOA$ would be the combination of Gaussian distribution, $T_d + T_{sh} + n$, and the distribution of the synchronization offset T_{sy} . Due to the unpredictable synchronization distribution, the overall distribution would be unpredictable as well.

B. Definition of DTDOA

DTDOA is defined as the difference of TDOAs for the target and RN between the same pair of ANs. Figure 1(a) illustrates the operation of DTDOA. Compared to a TDOA system, a RN is added to compensate for imperfect synchronization. In this subsection, we analyze the relation between TDOA and DTDOA in an ideal case, i.e., with perfect synchronization and no multipath propagation.

First, the TDOA for the target between AN1 and AN2 in Figure 1(a) can be defined as,

$$TDOA_t = \frac{L_{t1} - L_{t2}}{c}, \quad (2)$$

where $TDOA_t$ is the TDOA for the target between AN1 and AN2, L_{t1} and L_{t2} are the distances from the target to AN1

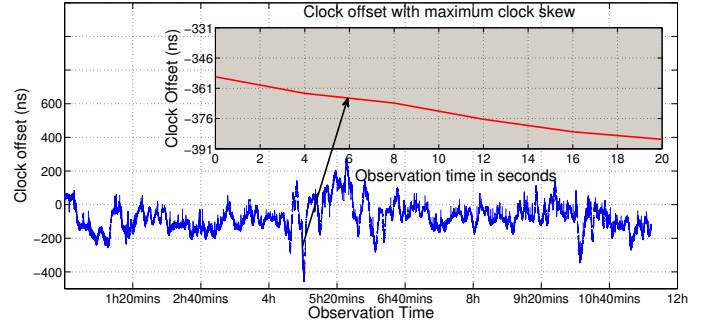


Fig. 2: GPS Synchronization

and AN2, and c is the speed of light. Second, the TDOA for the RN is,

$$TDOA_r = \frac{L_{r1} - L_{r2}}{c}. \quad (3)$$

where $TDOA_r$ is the TDOA for the RN between AN1 and AN2, L_{r1} and L_{r2} are the distances from the RN to AN1 and AN2.

Eventually, the DTDOA for the target and RN between AN1 and AN2 can be expressed as,

$$\begin{aligned} DTDOA &= TDOA_t - TDOA_r \\ &= \frac{(L_{t1} - L_{t2}) - (L_{r1} - L_{r2})}{c}. \end{aligned} \quad (4)$$

where $DTDOA$ denotes the DTDOA. If the RN is set in the center of the triangle, $TDOA_r$ would be zero, and hence the DTDOA would be the same as TDOA.

C. DTDOA Model in Reality

Based on the TDOA model as Equation (1) and the definition of DTDOA, we can construct a model for DTDOA considering a practical situation with multipath propagation and synchronization offset. The TDOA models for the target and RN can be respectively defined as,

$$TDOA_t = T_{td} + T_{tsh} + T_{tsy} + n, \quad (5)$$

$$TDOA_r = T_{rd} + T_{rsh} + T_{rsy} + n, \quad (6)$$

where T_{td} , T_{tsh} and T_{tsy} are respectively distance component, shadowing and multipath component, and synchronization offset component for the target; T_{rd} , T_{rsh} and T_{rsy} are for the RN.

Assuming the RN is set in the center of the triangle with $T_{rd} = 0$, DTDOA can be calculated as,

$$\begin{aligned} DTDOA &= TDOA_t - TDOA_r \\ &= T_{td} + (T_{tsh} - T_{rsh}) + (T_{tsy} - T_{rsy}) + n. \end{aligned} \quad (7)$$

Since the synchronization components T_{tsy} and T_{rsy} introduce an unpredictable influence to the DTDOA estimation, we would like to eliminate those components.

D. DTDOA with GPS Synchronization

In order to analyze the influence of synchronization effects on DTDOA, we first define the relative clock offset between two ANs as follow,

$$\Delta C(t) = \Delta f(t) \cdot t + \theta \quad (8)$$

where $\Delta C(t)$ is the relative clock offset between two ANs, $\Delta f(t)$ is the relative clock skew and θ is the initial clock offset, which is constant. In a short period, e.g., tens of seconds, the clock skew can be treated as constant and defined as $\Delta f(t) = \Delta f$. Therefore, Equation (8) can be rewritten as,

$$\Delta C(t) = \Delta f \cdot t + \theta \quad (9)$$

When the ANs receive a packet from the RN, the synchronization component for the RN can be defined as,

$$T_{rsy} = C(t_1) = \Delta f \cdot t_1 + \theta. \quad (10)$$

where t_1 is the time when the packet from the RN arrives at the ANs. After time I_{TR} the packet from the target arrives at the ANs and the synchronization component for the target can be defined as,

$$T_{tsy} = C(t_1 + I_{TR}) = \Delta f \cdot (t_1 + I_{TR}) + \theta. \quad (11)$$

Hence, the accumulated synchronization offset within the duration of I_{TR} can be calculated as,

$$T_{tsy} - T_{rsy} = \Delta f \cdot I_{TR}. \quad (12)$$

As shown in Figure 2, we have determined that although the GPS synchronization offset between two ANs can be as large as $200ns$, the relative clock skew is very small. The maximum relative clock skew of GPS synchronization we measured is about $15ns$ in ten seconds, i.e. $\Delta f = 1.5 \cdot 10^{-9}$. Therefore, if we set I_{TR} to few seconds, the accumulated synchronization offset ($T_{tsy} - T_{rsy} = \Delta f \cdot I_{TR}$) can be ignored. In our measurements with $I_{TR} = 1s$ the accumulated GPS synchronization offset ($T_{tsy} - T_{rsy}$) is smaller than $1.5ns$, allowing us to assume $T_{tsy} - T_{rsy} = 0$. Finally, we can obtain the DTDOA as,

$$DTDOA = T_{td} + (T_{tsh} - T_{rsh}) + n. \quad (13)$$

In the proposed DTDOA model the time-variant synchronization component is eliminated and only space-determined components are present. Furthermore, the distribution of the DTDOA is Gaussian with mean value of $T_{td} + (T_{tsh} - T_{rsh})$. As a result, the proposed DTDOA ranging is very suitable for localization.

IV. SUB-SAMPLE TIMESTAMP ESTIMATOR

As mentioned in section II-B, sub-sample timestamps with high resolution are the essential precondition to acquire accurate TDOA. In this section, an advanced method is proposed to achieve sub-sample timestamps with nanosecond resolution by using timing information from the signal processing chain.

In an ideal system, where the transmitter and receiver are perfectly synchronized, timestamps are taken at the optimal sampling moment of a symbol as shown in Figure 3. In the case of a GMSK modulation system, as applied in GSM, the signal is shaped by a Gaussian filter and thus the optimal sampling

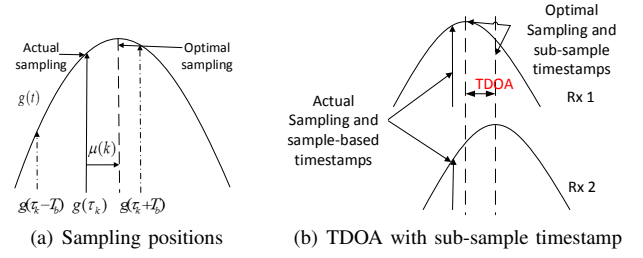


Fig. 3: Time recovery and sub-sample timestamp

position is at the peak of the Gaussian pulse $g(t)$. Denoting the sampling phase by τ_k , sampling would be on the peak of the pulse when $g(\tau_k - T_b) = g(\tau_k + T_b)$, where T_b is the symbol interval. The reason for this is the symmetric shape of the Gaussian pulse [12].

In practical systems, however, the receiver is not synchronous with the incoming data due to free running oscillators of the Digital-to-Analogue Converter (DAC) at the transmitter and the Analogue-to-Digital Converter (ADC) at the receiver. This results in suboptimal sampling, i.e., the actual sampling position is often before (as in Figure 3) or after the peak, displaced at $\mu(k)$. $\mu(k)$ is the normalized timing error given by,

$$\mu(k) = \frac{\Delta T(k)}{T_s}, \quad (14)$$

where $\Delta T(k)$ is the offset between actual and optimal sampling position and T_s is the constant sampling interval. The suboptimal sampling process would influence the accuracy of the sample-based timestamp because it can not distinguish time differences within one symbol duration. Therefore, we propose to consider the shift in the sampling position to achieve an accurate sub-sample timestamp, as shown in Figure 3(b).

To correct for shift in the sampling position during signal recovery, the time recovery method [12] is used. The method synchronizes the sampler with the pulses of the received analogue waveform. The sample stream is fed into a Timing Error Detection (TED) module to extract the timing error information between the actual and optimal sample positions. The timing error information is passed to a loop filter, which outputs the normalized timing error $\mu(k)$ to decide on the correction of the sampling time in the re-sampler. Subsequently, the sampling position can be adjusted to be closer to the optimal one.

We propose to apply the normalized timing error $\mu(k)$ of sample k to design a sub-sample timestamp. Once the receiver starts to receive packets and generate samples, we can count the generated samples and obtain the sample-based timestamp $T'(k)$ for the k th sample as follows [9],

$$T'(k) = T'(1) + T_s * (k - 1), \quad (15)$$

where $T'(1)$ is the sample-based timestamp for the first sample. In Equation (15) the resolution of the sample-based timestamp is limited by T_s . With the $\mu(k)$ obtained by the time recovery, we can improve the resolution as,

$$T(k) = T'(k) + \mu(k) \cdot T_s, \quad (16)$$

where $T(k)$ is the sub-sample timestamp. Now, assuming that the k th sample in the sample stream is the first sample of a received packet, $T(k)$ is the sub-sample timestamp for this packet. We propose to apply the sub-sample timestamp $T(k)$ in a narrow-band system (GSM) for localization.

V. SYSTEM REALIZATION AND SETUP

This section first discusses the implementation of the localization system using Software Defined Radio (SDR) and subsequently presents the deployment of the system for experimentation.

A. System Realization

The Universal Software Radio Peripheral (USRP) is implemented for the signal emitters (RN and target) with model E110 and receivers (ANs) with model N210. Both models rely on a RF frontend for transmitting and receiving analogue signals, ADC and DAC for analogue and digital signal conversion, and a Field Programmable Gate Array (FPGA) to control the sampling process. The USRP E110 is an embedded device which runs signal processing in an embedded ARM processor and is convenient for deployment and movement flexibility. Compared to E110, the USRP N210 can achieve higher processing capability but it needs to connect over a Gigabit Ethernet to a powerful machine, where the signal processing is done.

In order to represent the GSM signal with 271KHz symbol rate, we constructed our own transmitter to continuously generate GMSK-modulated signals with 250KHz symbol rate, which should be an integer divisor of the clock rate in ADC and DAC, 100MHz . The E110 is used to implement the transmitters. The receivers are implemented using the N210 model and the GNU Radio for signal processing. Before entering the signal processing chain in GNU Radio, the analogue signal is captured at the RF frontend and sampled at 100MHz by the ADC. In the FPGA, the data is downsampled to the required sampling frequency. In our case of 250KHz symbol rate and oversampling rate of 2, the required sampling rate is 500KHz and the corresponding sampling interval is $2\mu\text{s}$ (T_s in Equation (15)). Additionally, all the ANs are synchronized by GPS receivers.

Sample-based timestamps can be obtained by the clock in the FPGA. As mentioned earlier, the sample-based timestamp is limited in resolution by the sampling rate. In order to calculate our proposed sub-sample timestamp, we need to ensure that the normalized timing error $\mu(k)$ is associated to each sample. Therefore, we introduce certain modifications to the SDR signal processing chain. We make use of a mechanism called stream tags, provided in GNU Radio to attach tags with control information to the samples in the stream. To calculate the sub-sample timestamp, we need to attach the value of $\mu(k)$ for each sample as well as the number of the sample, k , in the sample stream and mark the beginning sample of each packet.

B. Measurement Setup

We conducted experiments in three types of environments, i.e., sub-urban with open space, urban with high building density, and indoor environments. The sub-urban measurements

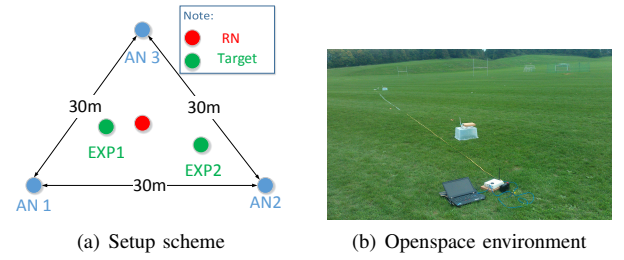


Fig. 4: Sub-urban measurements with open space, 3 ANs

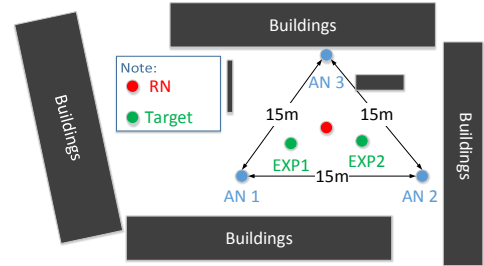


Fig. 5: Urban measurements in inner courtyard, 3 ANs

were taken in a football field (Figure 4) to minimize the influence of multipath propagation. The urban measurements were taken in an inner courtyard (Figure 5) and indoor environments were taken within a single conference room with dimensions of $7\text{m} \times 10\text{m}$. The choice of various environments allows us to analyze the influence of multipath propagation incrementally.

Two types of setup scenarios were used. In the first case only two ANs were deployed to mainly focus on evaluating the timestamp accuracy achievable with TDOA and DTDOA. In the second case three ANs were deployed as shown in Figure 4(a), which allows us to evaluate the localization accuracy achievable with multilateration besides TDOA and DTDOA ranging. Independently of the setup there was always a RN introduced to support the calculation of DTDOA, and the packet interval between RN and target, I_{TR} , is set to one second.

VI. LOCALIZATION ACCURACY ANALYSIS

We will first discuss our findings in the case of a sub-urban environment, followed by analysis on results for urban and indoor environments. Hence, we can gradually introduce the impact of multipath propagation. In all measurements we construct the Probability Density Function (PDF) of the TDOA and DTDOA values, collected during the experiments. By comparing the most frequently appearing value in the distribution with the actual value defined by the experiment's geometry, we can determine the accuracy of each technique.

A. Sub-Urban Open Space Environment

The TDOA and DTDOA ranging errors, which is defined as the difference between the estimated distance and the actual distance, are summarized in Table I; S stands for 'sub-urban'. With deployment of two ANs there is only one pair of ANs (AN 1 and AN 2), for which we can calculate the TDOA

and DTDOA. With deployment of three ANs we can run calculations for three pairs of ANs, as indicated in the table. We notice that TDOA performs worse than DTDOA. Imperfect synchronization for TDOA leads to larger errors from $5m$ to $47m$ with an average of $24.4m$. After introducing a RN in the system to compensate for synchronization offset, the performance of DTDOA is much more accurate, i.e., most location errors are within $10m$ with a mean value of $6.7m$. Furthermore, we are able to make estimations on the timestamp accuracy, thanks to the limited presence of multipath propagation in open space environments. Under such circumstances, by analyzing the DTDOA performance, we determined an average timestamp accuracy of $22ns$.

TABLE I: Ranging errors for sub-urban environment

| 3-AN deployment | | | | |
|-------------------|------------|-----------|-----------|-----------|
| Experiment Number | Algorithms | AN1 and 2 | AN2 and 3 | AN1 and 3 |
| Experiment S1 | TDOA | 5.6m | 22.6m | 23.1m |
| | DTDOA | 5.2m | 6.4m | 1.2m |
| Experiment S2 | TDOA | 5.5m | 39m | 33.5m |
| | DTDOA | 12.5m | 12m | 2m |
| 2-AN deployment | | | | |
| Experiment S3 | TDOA | 17m | | |
| | DTDOA | 8m | | |
| Experiment S4 | TDOA | 47m | | |
| | DTDOA | 6m | | |

In order to explain how the ranging error is calculated and to gain more insights into the behaviors of TDOA and DTDOA, we further analyze experiment S1. The PDF of the TDOA values is shown in Figure 6, while the PDF of DTDOA is shown in Figure 7. We want to calculate the ranging errors given in Table I. We take the most frequent value in the distribution and calculate the corresponding estimated distance. The results are compared with the actual distances for different pairs of ANs.

Returning to the PDF graphs, we easily observe that the remaining synchronization offset for TDOA leads to non-Gaussian distribution of the TDOA values. Recall that with perfect synchronization the TDOA distribution should have a Gaussian form. The fact that the DTDOA distribution fits closer to a Gaussian distribution indicates that the influence of the imperfect synchronization is eliminated and only the effect of Gaussian noise is present in the DTDOA value. This observation is in accordance with the analytical argumentation on the DTDOA model in Section III. Furthermore, the variance of the TDOA value is larger than the variance of DTDOA because the TDOA synchronization component introduces additional variance on top of the noise.

Furthermore, we applied the TDOA and DTDOA measurements to evaluate the performance of multilateration for open spaces. For TDOA-based multilateration, shown in Figure 8, we are not able to determine an intersection of the TDOA curves within the $30m \times 30m$ area of the experiment. The remaining synchronization offset introduces too large timing error for the TDOA value to allow for accurate multilateration. After eliminating the synchronization offset in DTDOA the localization error is about $6m$ for experiment S1 and $11m$ for experiment S2 as shown in Figure 9.

Based on the results for the sub-urban measurements, we can conclude that, by improving the timestamp accuracy and eliminating the remaining synchronization offset, we are

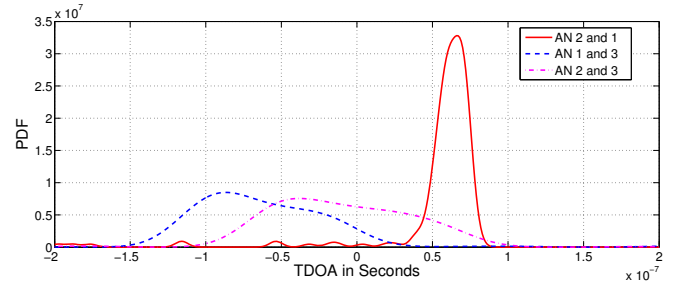


Fig. 6: TDOA for experiment S1

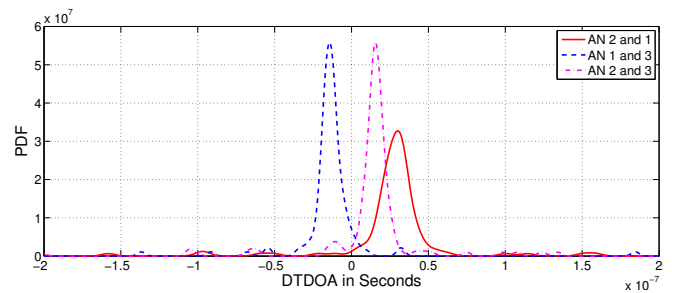


Fig. 7: DTDOA for experiment S1

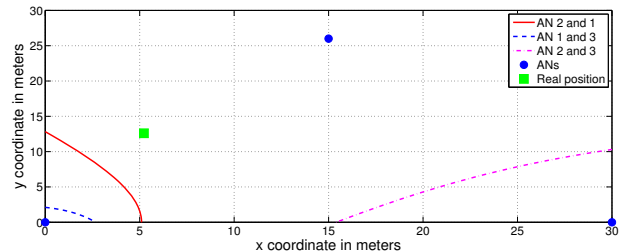


Fig. 8: TDOA multilateration for experiment S1

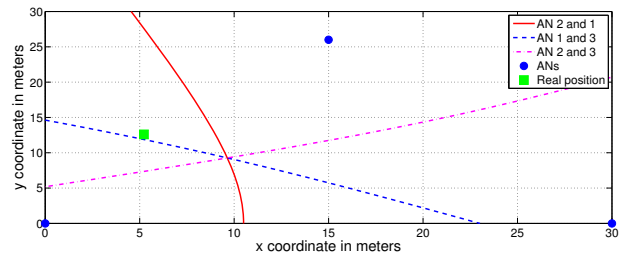


Fig. 9: DTDOA multilateration for experiment S1

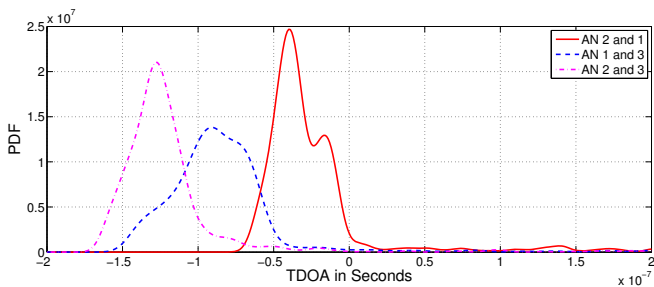


Fig. 10: TDOA for experiment U1

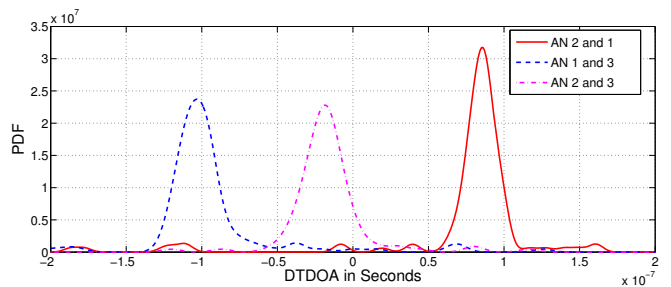


Fig. 11: DTDOA for experiment U1

able to achieve GSM ranging errors within $10m$. Hence, the DTDOA method outperforms TDOA and delivers very reasonable localization performance with multilateration.

B. Urban Environment

In order to introduce a stronger multipath propagation component we conducted another outdoor experiment but in an urban environment with high building density. The measurement setup is shown in Figure 5. An overview of the measured ranging errors is given in Table II, with U standing for 'urban'. Compared to the performance of TDOA with an average ranging error of $25.9m$, DTDOA benefits from eliminating the synchronization offset and reaches an average ranging error of $16m$. Clearly, moving to urban spaces degrades the performance of time-based localization as we see in the increased ranging error for DTDOA compared to the sub-urban case. The effect is explained with the presence of nearby buildings and other obstacles that contribute to a stronger multi-path propagation. Consequently, the DTDOA ranging error larger than $15m$ (the distance between two ANs) prevents us from applying the multilateration algorithm due to geometric limitations.

TABLE II: Ranging errors for urban environment

| Experiment Number | Algorithms | AN1 and 2 | AN2 and 3 | AN1 and 3 |
|-------------------|------------|-----------|-----------|-----------|
| Experiment U1 | TDOA | 21.25m | 43.15m | 18.4m |
| | DTDOA | 17.25m | 7.15m | 24.4m |
| Experiment U2 | TDOA | 32.7m | 37.4m | 2.2m |
| | DTDOA | 9.3m | 14.9m | 23.2m |

Again zooming into a single experiment, i.e., experiment U1, we show the PDF of the TDOA and DTDOA values in Figures 10 and 11, respectively. Similar to the sub-urban scenario, the TDOA distribution deviates from a Gaussian distribution due to imperfect synchronization. The Gaussian distribution of the DTDOA, however, demonstrates that also in urban settings the DTDOA method is able to eliminate the influence of any remaining synchronization offset. Accordingly, the variance of the DTDOA distribution is smaller than the variance of the TDOA distribution.

In conclusion, DTDOA ranging can eliminate synchronization offsets and achieves average accuracy of $16m$, which is around 40% more accurate than TDOA. Furthermore, multipath propagation in dense building environments degrades the localization accuracy.

C. Indoor Environment

In a final step, we took measurements in an indoor environment, indicated by I in the experiment notation. We used the single conference room, characterized with LOS propagation but stronger multipath propagation compared to the outdoor scenarios. The experiment allowed us to evaluate the performance of the proposed sub-sample timestamp under complex propagation conditions. Our findings on the ranging error are summarised in Table III for both TDOA and DTDOA measurements. DTDOA with an average ranging error of $17.3m$ demonstrates about 50% better performance compared to TDOA with average ranging error of $36.2m$. The results confirm our expectation that narrow-band signals are susceptible to multipath propagation, which introduces distortions in the pulse shape and thus deteriorates the accuracy of the taken timestamp. Again, as in the urban case, the use of multilateration is not feasible indoor. Observations on the distributions of both the TDOA and DTDOA values are in line with the previous two experiments.

The results for indoor spaces led us to conclude that the accuracy of TDOA/DTDOA-based localization with narrow-band signal for indoor spaces is strongly influenced by multipath propagation and acceptable accuracy below $10m$ requires the development of compensation methods for the multipath propagation effect.

TABLE III: Ranging errors for indoor environment

| Experiment Number | Algorithms | AN1 and 2 | AN2 and 3 | AN1 and 3 |
|-------------------|------------|-----------|-----------|-----------|
| Experiment I1 | TDOA | 42.9m | 26m | 65.9m |
| | DTDOA | 35.4m | 7m | 30.9m |
| Experiment I2 | TDOA | 16m | 10.2m | 48.2m |
| | DTDOA | 13m | 22.8m | 9.8m |
| Experiment I3 | TDOA | 58.9m | 2.9m | 61.8m |
| | DTDOA | 37.9m | 10.1m | 28.8m |
| Experiment I4 | TDOA | 17.3m | 31m | 53.3m |
| | DTDOA | 4.3m | 1m | 6.3m |

VII. CONCLUSIONS

The focus of this paper is evaluation of time-based localization with narrow-band signals. For practical evaluations we consider GSM signals, GPS node synchronization (needed in time-based localization) and the commonly preferred TDOA positioning technique. The performance of TDOA depends on two factors, synchronization between the anchor nodes and accuracy of the taken timestamp. We propose improvements to both.

The paper contributed: (i) a method to compensate for imperfect node synchronization, (ii) a method to calculate a sub-sample timestamp with accuracy in nanoseconds, and (iii) evaluations of localization accuracy in sub-urban, urban and indoor environments. First, we proposed to use Differential TDOA with a reference node and GPS synchronization to eliminate the effect on imprecise synchronization. Our method outperforms others with its practical ease because no strict parametrization of the reference node is needed, as in other proposals. Second, we introduced a sub-sample timestamp with nanoseconds accuracy. In the construction of the timestamp we used fine-grain timing information from the signal processing chain. Finally, we demonstrated the increase in localization accuracy, achieved by the proposed improvements compared to TDOA. We showed that by using DTDOA combining GPS synchronization and sub-sample timestamps we were able to reach localization accuracy of around $10m$ for open spaces.

Evaluations of the localization accuracy were done for three different environment types, namely, sub-urban with open space, urban and indoor. Our findings showed that the proposed DTDOA method can successfully eliminate the effects of imprecise synchronization and increase the achievable accuracy of ranging as much as 50%. We also demonstrated that the strong multipath propagation indoors deteriorates the accuracy of localization and challenges the use of multilateration techniques. In our view, further improvements in the localization accuracy with narrow-band signal require the development of methods able to isolate the effect of multipath propagation on the timestamp accuracy.

REFERENCES

- [1] H. Liu, H. Darabi, P. Banerjee, and J. Liu, "Survey of wireless indoor positioning techniques and systems," *Systems, Man, and Cybernetics, Part C: Applications and Reviews, IEEE Transactions on*, vol. 37, no. 6, pp. 1067–1080, 2007.
- [2] Y.-C. Wu, Q. Chaudhari, and E. Serpedin, "Clock synchronization of wireless sensor networks," *Signal Processing Magazine, IEEE*, vol. 28, no. 1, pp. 124–138, 2011.
- [3] D. Dardari, A. Conti, U. Ferner, A. Giorgetti, and M. Win, "Ranging with ultrawide bandwidth signals in multipath environments," *Proceedings of the IEEE*, vol. 97, no. 2, pp. 404–426, 2009.
- [4] Z. Li, D. Dimitrova, T. Braun, and D. Rosario, "Highly accurate evaluation of gps synchronization for tdoa localization," in *Wireless Days (WD), 2013 IFIP*, Nov 2013, pp. 1–3.
- [5] W. Liu and K. Dostert, "Development and application of gps-based time synchronization in power line channel characterization," in *Fifth Workshop on Power Line Communications*, 2011.
- [6] F. Winkler, E. Fischer, E. Grass, and P. Langendorfer, "An indoor localization system based on dtdoa for different wireless lan systems," in *3rd Workshop on Positioning, Navigation and Communication*, 2006.
- [7] A. Nagy, R. Exel, P. Loschmidt, and G. Gaderer, "Time-based localisation in unsynchronized wireless lan for industrial automation systems," in *Emerging Technologies Factory Automation (ETFA), 2011 IEEE 16th Conference on*, 2011, pp. 1–8.
- [8] S. Ganerwal, R. Kumar, and M. B. Srivastava, "Timing-sync protocol for sensor networks," in *Proceedings of the 1st International Conference on Embedded Networked Sensor Systems*, ser. SenSys '03. ACM, 2003, pp. 138–149.
- [9] G. Nychis, T. Hottelier, Z. Yang, S. Seshan, and P. Steenkiste, "Enabling mac protocol implementations on software-defined radios," in *Proceedings of the 6th USENIX Symposium on Networked Systems Design and Implementation*, ser. NSDI'09. USENIX Association, 2009, pp. 91–105.
- [10] L. Zimmermann, A. Goetz, G. Fischer, and R. Weigel, "Gsm mobile phone localization using time difference of arrival and angle of arrival estimation," in *Systems, Signals and Devices (SSD), 2012 9th International Multi-Conference on*, 2012, pp. 1–7.
- [11] TechnoCom, "Trueposition indoor location test bed report," Tech. Rep., 2013.
- [12] M. Heinrich, M. Moeneclaey, and S. Fechtel, *Digital Communications Receivers: Synchronization, Channel Estimation and Signal Processing*. John Wiley and Sons, 1998.